

Morphological features of lung white spots based on the Otsu and Phansalkar thresholding method

Retno Supriyanti¹, Syadzwina Luke Dzihniza¹, Muhammad Alqaaf², Muhammad Rifqi Kurniawan¹,
Yogi Ramadhani¹, Haris Budi Widodo³

¹Department of Electrical Engineering, Jenderal Soedirman University, Purwokerto, Indonesia

²Department of Information Science, Nara Institute of Science and Technology, Ikoma, Japan

³Department of Dentistry, Jenderal Soedirman University, Purwokerto, Indonesia

Article Info

Article history:

Received Oct 20, 2023

Revised Nov 9, 2023

Accepted Nov 17, 2023

Keywords:

COVID 19

Otsu thresholding

Phansalkar thresholding

Segmentation

X-ray thorax

ABSTRACT

COVID-19 is a disease that causes respiratory system disorders, so various tests are needed. One of them uses a chest X-ray or thorax. A chest X-ray will depict the lungs as a whole so that patches like white shadows will be visible. In this study, the number of lung areas and white spots can be observed and detected using segmentation techniques in image processing. But before entering the segmentation stage, the image will go through the preprocessing stage using the tri-threshold fuzzy intensification operators (fuzzy IO) method. It then segmented the lungs using the Otsu method by changing the digital image from grey to black and white based on comparing the threshold value with the pixel colour value of the digital image. Then, further segmentation was carried out using the Phansalkar method to detect and simultaneously count the number of white spots. Referring to the experiments we have carried out, Otsu Phansalkar's segmentation performance promises to be developed further.

This is an open access article under the [CC BY-SA](https://creativecommons.org/licenses/by-sa/4.0/) license.



Corresponding Author:

Retno Supriyanti

Department of Electrical Engineering, Jenderal Soedirman University

Jl. HR. Boenjamin 708, Purwokerto, Indonesia

Email: retno_supriyanti@unsoed.ac.id

1. INTRODUCTION

COVID-19 is a disease that causes respiratory system disorders caused by the severe acute respiratory syndrome coronavirus virus. The Coronavirus can cause mild respiratory system conditions, severe lung infections, and even death. In the early phase of the disease, COVID-19 can resemble flu symptoms; symptoms can disappear and heal or even worsen. The Coronavirus can attack anyone, so it spreads very quickly. According to data released by the World Health Organization, the number of confirmed positive cases globally in 216 countries has reached 14,043,176 people with a total death of 597,583 people, so the global case fatality rate due to COVID-19 is around 4.1% and is still increasing [1]. Determining the diagnosis and severity of a patient infected with COVID-19 can be done with complete hematology, rapid tests, and PCR tests. However, additional tests are needed to diagnose the infection's severity more precisely, thoroughly, and efficiently. One of them can be done with a chest X-ray examination. A chest X-ray is an examination using electromagnetic radiation to display an image of the inside of the chest so that it can detect inflammation in the lungs. The output of the X-ray is an image with X-rays, which is then used for observation.

From the literature search, much research is currently discussing COVID-19 based on image processing techniques. Noviasari and Mashoedah [2] classify chest X-ray images for coronavirus infection based on the internet of things (IoT) using the Sobel operator, which is connected in real-time. Gupta and Agrawal [3] classify chest X-ray images for coronavirus infection based on the IoT using the Sobel operator,

which is connected in real-time to the Internet. Shakouri *et al.* [4] present an open-access repository of over 1,000 computerized tomography (CT) images of the lung acquired since the start of the COVID-19 pandemic, which can serve as a starting point for more comprehensive database models. Besides that, it can also be used as a reference source for radiology training in rural areas. Kazem *et al.* [5] discuss using three-dimensional convolutional neural networks to analyze medical images. Their paper discusses the preprocessing steps for medical images and then uses the model. The target is to use low-resolution to high-resolution images using TensorFlow. Pranolo and Mao [6] proposed a method for feature extraction and classification of COVID-19 by integrating the deep CNN method with an autoencoder (AE) called CAE-COVIDX. Kumar *et al.* [7] proposed a new method by combining the zernike moment feature (ZMF) algorithm with the gray level co-occurrence matrix feature (GF) in performing feature extraction in COVID-19 infection. The algorithm they use is 36 ZMF and a texture with variance and contrast variables. Khorami *et al.* [8] proposed a method for segmenting the chest area using a combination of graylevel cooccurrence matrix (GLCM) and discrete wavelet transform (DWT). Furthermore, they also optimized the convolutional neural network (CNN) algorithm for image classification based on the features that had been successfully extracted.

Rasheed [9] proposed a hybrid method based on artificial intelligence in detecting and controlling COVID-19. The first step is to remove noise from the image using a conservative method, then perform feature extraction using linear discriminant analysis (LDA) and principal component analysis (PCA). Finally, they classify with a CNN, support vector machine (SVM), and logistic regression (LG). Ahsan *et al.* [10] developed a chest X-Ray image-based detection of COVID-19 by carrying out feature extraction and classification based on histogram-oriented gradient (HoG) and CNN algorithms. Subramaniam *et al.* [11] proposed detecting COVID-19 and pneumonia by combining the HoG method, Haar transformation, and local binary pattern (LBP) to extract essential features in lung images. Chen *et al.* [12] developed the ensemble CNN method combined with several trained CNN models with the most sampling strategy in the classification of COVID-19 based on chest X-ray images. Taresh *et al.* [13] proposed a CNN method called KL-MOB by adding Kullback–Leibler (KL) in image processing-based COVID-19 detection. Sampath *et al.* [14] has evaluated the development of techniques based on generative adversarial neural networks (GANs) in overcoming the problem of image data imbalance. Elzeki *et al.* [15] proposed a two-layer perceptual image fusion method using deep learning to obtain more informative chest X-ray images to be used as COVID-19 datasets. Nassif *et al.* [16] suggested using sound and image signals in COVID-19 detection. They have carried out experiments using deep learning methods based on sound signals, image signals, and a combination of sound and image signals.

Danapaquame *et al.* [17] discussed image processing techniques and analysis related to COVID-19, including image processing techniques, segmentation, diagnosis, and follow-up based on traditional methods to evaluate the entire discussion. Siddiqui *et al.* [18] proposed using the ultra wide-band radar method temporally in the early detection of chronic lung disease. Aswathy *et al.* [19] used nano images enhanced with Gabor filters and histogram equalization in the early detection of lung cancer based on the guaranteed convergence particle swarm optimization (GCPSO) algorithm. In our previous research [20]–[23], we segmented the image of the lung area, including the white spots in it, in COVID-19 patients using the Bradley and Sauvola method. Unfortunately, the performance of this segmentation method still needs to be improved. So, in this paper, we will discuss using the Otsu and Phansalkar Thresholding method. The Otsu method is a global thresholding method for digital image segmentation that can automatically generate threshold values for digital images with the criteria of linear discriminant analysis of histogram grey levels.

Meanwhile, the Phansalkar thresholding method is included in the adaptive local thresholding method, a development of the Sauvola and Pietikainen methods. The Phansalkar method aims to develop a suitable method for a problem: obtain more accurate segmentation results by getting higher threshold values and accurate binary results [24]. To the best of our knowledge, using this method in early screening for lung abnormalities is the first, so we emphasize this as a novelty in this paper.

2. PROPOSED METHOD

The method we use in this experiment is the Otsu and Phalsakar Thresholding method. The process begins by entering digital chest X-ray images of patients suffering from COVID-19 in RGB color space into the system. The image will go through a resizing process by changing the image size to 500×500 pixels, then enter the preprocessing stage. At this stage, color stretching is carried out on the image and equalization of the histogram in the fuzzy domain using the fuzzy intensification operator method. Then, the preprocessing results will go through a cropping stage according to the region of interest using the polygonal cropping method.

Next, carry out the first lung area segmentation using the Otsu thresholding method. This method will calculate the minimum value of the pixel level on each side of the threshold to find the threshold value. In the process, each image pixel will be classified with a certain threshold. If the pixel value is less than the threshold, it will have a value of 0, and if it is more or equal to the threshold, it will have a value of 1. So that

we get a separation between the foreground and background, the postprocessing process will measure the object parameters and produce information in the form of the area of the lungs, diameter, perimeter, and centroid. The second segmentation is the segmentation of the area of white spots using the Phansalkar thresholding method. This method will find a local mean and standard deviation value better than the Sauvola method by adapting the local threshold value according to the contrast in the pixel environment. When there is high contrast on one side of the image, the mean and standard deviation values will be the same as the dynamic range of the standard deviation to normalize the image. Meanwhile, when the contrast is low, the value of the threshold becomes below the average. Thus, it can remove relatively dark background areas. So, we will get a segmentation of the white spots. Then, in the postprocessing process, we will measure object parameters such as diameter, perimeter, and centroid. So, the system can perform calculations and produce information in the form of lung area, area of white spots, number of white spots, and percentage of white spots.

3. METHOD

3.1. Input image

We use images from X-ray machine modalities. An X-ray of the lungs will be able to describe the presence of infiltrates or fluid in the lungs and detect the presence of coverings, which indicate inflammation due to infection from a virus. In patients with mild infections, the changes in X-ray results are not too different from normal lungs. Meanwhile, the X-ray picture will look different in patients with severe infections. Table 1 shows characteristic differences between X-ray images of the lungs in patients with COVID-19 who have mild, severe, and critical conditions and those of normal lungs [25].

Table 1. Table of differences between the characteristics of X-ray images of COVID-19 lungs and normal lungs

No	Lung category	X-ray image	Characteristics
1	Normal		<ul style="list-style-type: none"> – The shape, size, and tissue of the lungs look normal – The shape and location of the diaphragm looks normal – The lungs appear dark or black all over – The heart silhouette is visible – No abnormal build-up of fluid or air is seen, and no foreign body is seen
2	Mild COVID-19		<ul style="list-style-type: none"> – The lungs still look a bit black – Inflammation in the lungs begins to appear – The lungs appear opaque with a shadow from GroundGlass Opacity, indicating fluid filling the lungs.
3	Severe COVID-19		<ul style="list-style-type: none"> – Spots or white areas on the lungs are no longer vague and look more apparent. – The white spots appear to have started to connect – The appearance of the lungs has started to look white on one side.
4	Critical COVID-19		<ul style="list-style-type: none"> – Accumulation of fluid and swelling has been thorough to almost all parts of the lungs so that the lungs look white on both sides. – The shape of the lungs is not visible or incomplete. – The heart silhouette is not visible. – The location of the diaphragm is not visible because it is covered with white spots.

X-rays are imaging-based diagnostic tests using electromagnetic wave radiation or X-rays that are emitted to the part of the body to be examined. On an X-ray, the image of solid objects such as bone or iron is displayed as white, while the air in the lungs appears black. An X-ray of the lungs will depict the presence of infiltrates or fluid in the lungs and detect any covering that indicates inflammation in the lungs due to infection from a virus [26].

3.1.1. Graphical user interface design stage

We use a graphical user interface (GUI) based on the MATLAB programming language at this stage. In this research, the author will create a GUI design for a Thorax X-ray image processing application using the GUIDE feature found in MATLAB R2019a software, as shown in Figure 1. In computing technology, a graphical user interface or APG is a type of user interface that uses graphical methods of interaction on electronic devices between the user and the computer. GUI displays objects that can convey information and represent user actions. With a GUI, we can know that what we input has been received and

the response is shown visually. The GUI can be seen from changes in color, size, visibility, and the like when an interaction occurs. By using this GUI, system typing is no longer needed. The existence of a GUI makes using software easier.

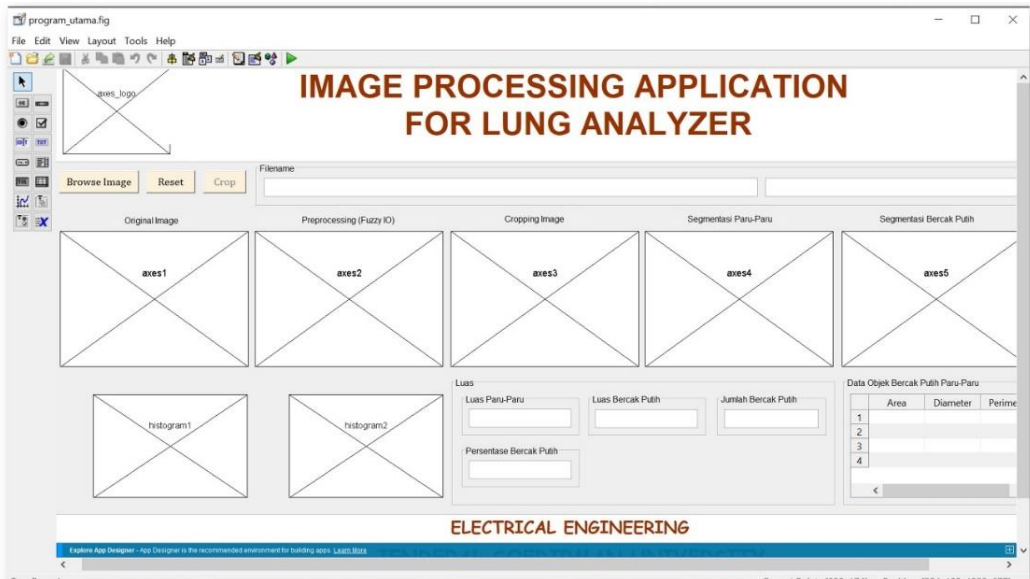


Figure 1. GUI design system

3.1.2. Design system

The system design stages are shown in Figure 2, where the diagram shows the outline of the system process that we have developed and the relationship between one stage and another. Users can interact with the system to either enter or retrieve data. The X-ray image is input, and the user manually carries out the process via the MATLAB GUI.

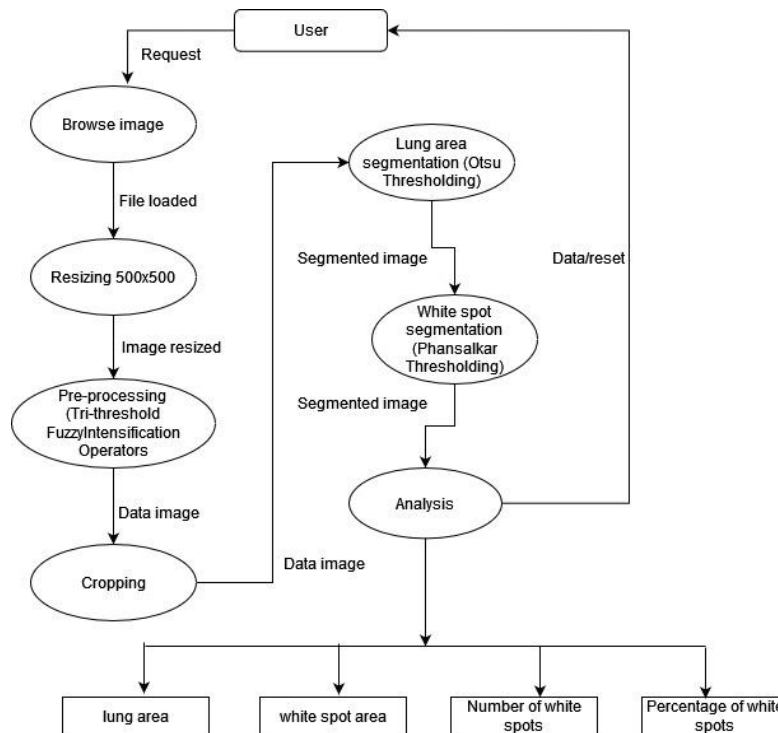


Figure 2. Flow diagram

The process begins by entering a digital chest X-ray image in RGB color space into the system. The image will resize by changing the image size to 500×500 pixels, then enter the preprocessing stage. At this stage, color stretching is carried out on the image and equalization of the Histogram in the fuzzy domain using the fuzzy intensification operator method. Then, the preprocessing results will go through a cropping stage according to the region of interest (RoI) using the polygonal cropping method. Using the Otsu thresholding method, the system will carry out the first lung area segmentation in the next stage. This method will calculate the minimum value of the pixel level on each side of the threshold to find the threshold value. Each image pixel will be classified with a certain threshold in the process. If the pixel value is less than the threshold, it will have a value of 0; if it is more or equal to the threshold, it will have a value of 1. So that we get a separation between the foreground and background, the postprocessing process will measure the object parameters and produce information in the form of the area of the lungs-lung, diameter, perimeter, and centroid. The second segmentation is the segmentation of the area of white spots using the Phansalkar thresholding method. This method will find a local mean and standard deviation better than the Sauvola method by adapting the local threshold value according to the contrast in the p environment. When there is high contrast on one side of the image, the mean and standard deviation values will be the same as the dynamic range of the standard deviation to normalize the image. Meanwhile, when the contrast is low, the value of the threshold becomes below the average. Thus, it can remove relatively dark background areas. So, the system will get a segmentation of the white spots. Then, in the postprocessing process, the object parameters will be measured, producing information in white spot area, diameter, perimeter, and centroid. So, the system can calculate and produce information in the form of lung area, area of white spots, number of white spots, and percentage of white spots.

3.1.3. Test and evaluation steps

At this stage, system testing will be carried out to determine the extent of the capabilities of the Otsu and Phansalkar methods in segmenting lung area and white spots in X-ray images and whether they are as expected or not. If the system cannot segment properly, the problem will be improved and re-assessed. The main purpose of this testing is to ensure that the resulting software meets previously determined requirements. The software testing process involves executing a software component or system using manual or automated tools to evaluate one or more properties of interest. The goal of software testing is to identify errors, gaps, or requirements that are missing or different from actual requirements. Defects found in the software can damage the system's reputation, leading to a loss of customer trust. Software testing allows us to create a system that meets or exceeds customer expectations, resulting in more sales and a larger market share. The software testing process is also necessary because if there are bugs or errors in the software, these problems can be identified early and resolved before the product is shipped to customers. Testing improvements can best be achieved by evaluating testing effectiveness on top of each software test implementation.

4. RESULTS AND DISCUSSIONS

Preprocessing is the initial stage carried out in digital image processing. This research will use resizing to make the image size uniform, then cropping to limit the research area, and use the Tuned Tri-threshold fuzzy intensification operator method to improve image quality. The resizing process is needed to normalize the image so that the research data has a uniform size and the process in the system becomes faster and more accurate. The image size of 500×500 pixels was chosen because the author has conducted resizing trials on the original and resized images. The results show that the original image's segmentation process has a longer duration than the resized image. However, the two have similar segmentation results. Sample comparison of resized and non-resized data is shown in Tables 2 and 3.

Table 2. Comparison of original size COVID-19 lung X-ray image test results with 500×500 resized images

No	Image	Original size		Resize 500×500	
		Percentage of test result	Test duration	Percentage of test results	Test duration
1	Covid_image_21	20.0691	1'01"	20.2716	29"
2	Covid_image_22	16.6172	1'17"	16.646	37"
3	Covid_image_23	33.0451	55"	33.8173	32"

Table 3. Comparison of the original size normal lung X-ray image test results with the 500×500 resize image

No	Image	Original size		Resize 500×500	
		Percentage of test result	Test duration	Percentage of test results	Test duration
1	Normal_image_21	12.7341	1'39"	14.1343	36"
2	Normal_image_22	16.9182	1'33"	16.3857	35"
3	Normal_image_23	19.2772	1'40"	17.313	37"

In image preprocessing, we use the tuned tri-threshold fuzzy intensification operator. The use of this method is to increase color sharpness in the image by improving image quality by smoothing the histogram. Figure 3 shows the difference between the original image histogram and the fuzzy IO results.

In Figure 3(a), the histogram of the original image shows the uneven color distribution, limited to a specific range, and skewed towards the left so that the image color is darker than the right side. In contrast, if the image skews towards the right, the image will be lighter. So, a good histogram can be seen in Figure 3(b), where the colors are well distributed throughout the range.

To get the region of interest, we cropped it to focus only on the lung using the polygonal cropping method. The main aim of using this technique is to simplify the segmentation process so that the detection process can be more focused, detailed, and optimal. Figure 4 shows the process of cropping the lung area using polygonal cropping in which Figure 4(a) shows the image before cropping, while in Figure 4(b), cropping has been done and only leaves the lung.

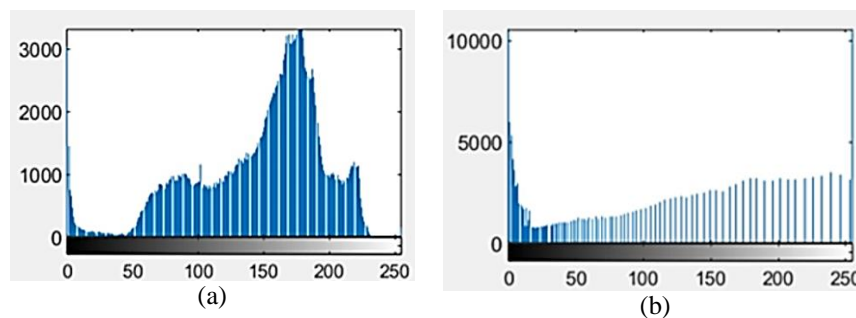


Figure 3. The difference between the original image histogram and the fuzzy IO results (a) original image histogram and (b) fuzzy IO histogram

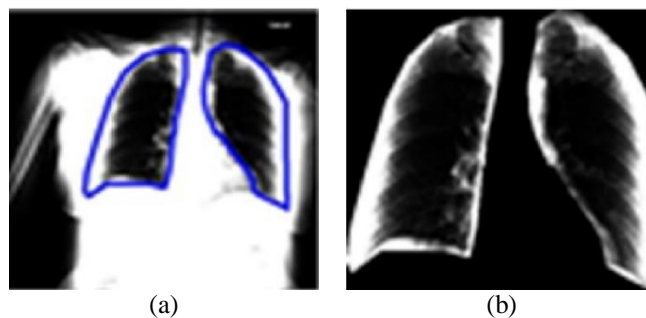


Figure 4. The process of cropping the lung area using polygonal cropping (a) cropping area and (b) cropping result

We use two segmentation methods at the segmentation stage: Otsu thresholding and Phansalkar thresholding. The Otsu method will perform a threshold search to be able to segment. After determining the threshold value, this method will automatically separate the foreground and background of the lung X-ray image. The results of lung segmentation using Otsu will be re-segmented using the Phansalkar method to detect white-spot objects. This method will segment the cropping results following the masking of the lung segmentation results by Otsu thresholding. So, only the white spots on the lungs will be segmented. Sample results of both segmentations on X-rays of COVID-19 lungs and normal lungs are shown in Tables 4 and 5.

Table 4. Example of COVID lung segmentation data

Image	Cropping image	Lung segmentation	White-spots segmentation
Covid_image_21			

Table 5. Example of normal lung segmentation data

Image	Cropping image	Lung segmentation	White-spots segmentation
Normal_image_21			

At the postprocessing stage, we use the labeling method. In each area of the segmented white spot object, the parameters such as centroid, area, perimeter, and marked using a red square label will be searched, then the system will process lung calculations including the number of lung areas, the number of white spots, and the total area of the white spotting object. Based on the data generated by the system, we calculate the percentage of white spots using (1). Sample data from the labeling results can be seen in Tables 6 and 7.

$$\text{Percentage of white spots} = \frac{\text{white spots area}}{\text{lung area}} \times 100\% \quad (1)$$

Table 6. Results of labeling COVID-19 lung image

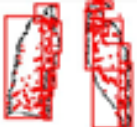
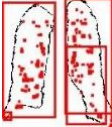
Image	Image of labelling result	Lung area (Pixel)	Image segmentation result	Number of white spots	Percentage of white spots
Covid_image_21		31711.9	6428.5	185	20.2716

Table 7. Result of labeling normal lung image

Image	Image of labelling result	Lung area (Pixel)	Image segmentation result	Number of white spots	Percentage of white spots
Normal_image_21		52177.1	7374.88	140	14.1343

We test with a test image to see whether it matches the program output results; testing was carried out with the hypothesis that the lung X-ray area of COVID-19 sufferers had a lung area smaller than the normal lung X-ray area, the area of white spots was more significant than the area of white spots on normal lung X-rays, the number of white spots was more significant than the number lung X-ray white spots are normal, and the percentage of white spots is higher than the percentage of normal lung white spots. However, after testing, several images' results did not match the hypothesis. This can be caused by poor or inappropriate image quality, such as low-quality X-ray machines or lack of accuracy in selecting X-ray data. Sample research results not by the hypothesis are shown in Tables 8 and 9.

Table 8. Anomaly X-ray image data of COVID-19 lung

Image	Image of labelling Result	Lung area (Pixel)	Image segmentation result	Number of white spots	Percentage of white spots	Test result
Covid_image_5		31576.8	682.625	101	2.16179	Failed

Table 9. Anomaly X-ray image data of normal lung

Image	Image of labelling result	Lung area (Pixel)	Image segmentation result	Number of white spots	Percentage of white spots	Test result
Normal_image_1		48317	12583.5	287	26.0436	Failed

Data anomalies show that the number and percentage of white spots in COVID-19 lung X-ray images are below the number and percentage of white spots in normal lung X-ray images. After segmentation using the Sauvola thresholding, Bradley thresholding, and Otsu-Phansalkar thresholding methods on 95 thorax X-ray image data, of which 45 data are thorax X-ray image data of patients suffering from COVID-19, and the other 50 data are chest x-ray image data of normal patients. This can be done comparison of test success rates as presented in Table 10.

Table 10. Performance of the Sauvola, Bradley, and Otsu-Phansalkar thresholding methods test results

Methods	Sauvola thresholding			Bradley thresholding			Otsu-phansalkar thresholding		
	Success	Failed	Success percentage	Success	Failed	Success percentage	Success	Failed	Success percentage
X-ray Covid images	32	13	71.11%	33	12	73.33%	35	10	77.78%
X-ray normal images	27	23	54%	25	25	54%	27	23	54%

Based on the results obtained in Table 10, each method has a different percentage of success. In the Otsu and Phansalkar Thresholding method, the test success rate for thorax X-ray images of patients suffering from COVID-19 was 77.78%, with the test success rate for thorax X-ray images of normal patients at 54%, in the Sauvola thresholding method, the test success rate for thorax X-ray images was obtained. Patients suffering from COVID-19 was 71.11%, with a test success rate on thorax X-ray images of normal patients of 54%, and using the Bradley thresholding method, the test success rate on thorax X-ray images of patients suffering from COVID-19 was 73.33% with a success rate tests on the patient's thorax X-ray images were expected at 54%.

5. CONCLUSION

The Otsu Thresholding and Phansalkar thresholding methods can segment lung objects and white spots in chest X-ray images. However, the quality of the original image greatly influences the segmentation process. When using this method, accuracy in the cropping process is needed because it can influence the segmentation results quite significantly. From the experimental results, calculating the percentage of white spots on chest X-ray images using the Otsu and Phansalkar thresholding methods, we obtained an average value of the percentage of white spots for patients suffering from COVID-19. It amounted to 19.01924% with a success rate of 77.78%, and the percentage of white spots for normal patients was 13.91139% with a success rate of 54%. Based on the results of comparing the average percentage of white spots in the two data, it was found that the difference between the percentage of white spots in the lungs for COVID-19 and normal was 5.10785%. So, the system has successfully tested the two types of data samples provided. Meanwhile, the data anomalies in the research can be caused by a need for more accuracy in image selection and the quality of the input images used.

ACKNOWLEDGEMENTS

This research was funded by the Ministry of Education, Culture, Research and Technology through the 2023 Basic Research Scheme with contract number 1554/UN23/PT.01.02/2023.

REFERENCES

- [1] World Health Organization, "Coronavirus disease (COVID-19)," *World Health Organization*, 2020.
- [2] L. Noviasari and Mashoedah, "Classification of thorax X-ray results on corona virus infection based on internet of things (IoT)," *Journal of Physics: Conference Series*, vol. 1737, no. 1, pp. 1–12, 2021, doi: 10.1088/1742-6596/1737/1/012001.
- [3] Y. K. Gupta and S. Agrawal, "A study of lung disease using image processing in big data environment," *IOP Conference Series: Materials Science and Engineering*, vol. 1022, no. 1, pp. 1–10, 2021, doi: 10.1088/1757-899X/1022/1/012030.
- [4] S. Shakouri *et al.*, "COVID19-CT-dataset: an open-access chest CT image repository of 1000+ patients with confirmed COVID-19 diagnosis," *BMC Research Notes*, vol. 14, no. 1, pp. 1–4, 2021, doi: 10.1186/s13104-021-05592-x.
- [5] R. A. Kazem, J. H. Suad, and H. A. Abdulbaqi, "Super-resolution using 3d convolutional neural networks in CT scan image of COVID19," *Turkish Journal of Computer and Mathematics Education (TURCOMAT)*, vol. 12, no. 12, pp. 4408–4415, 2021.
- [6] A. Pranolo and Y. Mao, "Cae-covidx: Automatic covid-19 disease detection based on X-ray images using enhanced deep convolutional and autoencoder," *International Journal of Advances in Intelligent Informatics*, vol. 7, no. 1, pp. 49–62, 2021, doi: 10.26555/ijain.v7i1.577.
- [7] K. G. S. Kumar, A. Venkatesan, D. Selvaraj, and A. N. J. Raj, "Rapid and accurate diagnosis of COVID-19 sases from chest X-ray images through an optimized features extraction approach," *Electronics (Switzerland)*, vol. 11, no. 17, 2022, doi: 10.3390/electronics11172682.

- [8] E. Khorami, F. M. Babaei, and A. Azadeh, "Optimal diagnosis of COVID-19 based on convolutional neural network and red fox optimization algorithm," *Computational Intelligence and Neuroscience*, vol. 2021, 2021, doi: 10.1155/2021/4454507.
- [9] J. Rasheed, "Analyzing the effect of filtering and feature-extraction techniques in a machine learning model for identification of infectious disease using radiography imaging," *Symmetry*, vol. 14, no. 7, 2022, doi: 10.3390/sym14071398.
- [10] M. Ahsan, A. Based, J. Haider, and M. Kowalski, "Fusion and deep learning," 2021.
- [11] U. Subramaniam, M. M. Subashini, D. Almakhles, A. Karthick, and S. Manoharan, "An expert system for COVID-19 infection tracking in lungs using image processing and deep learning techniques," *BioMed Research International*, vol. 2021, 2021, doi: 10.1155/2021/1896762.
- [12] Y. M. Chen, Y. J. Chen, W. H. Ho, and J. T. Tsai, "Classifying chest CT images as COVID-19 positive/negative using a convolutional neural network ensemble model and uniform experimental design method," *BMC Bioinformatics*, vol. 22, pp. 1–20, 2021, doi: 10.1186/s12859-021-04083-x.
- [13] M. M. Tareh, N. Zhu, T. A. A. Ali, M. Alghaili, A. S. Hameed, and M. L. Mutar, "KL-MOB: automated COVID-19 recognition using a novel approach based on image enhancement and a modified MobileNet CNN," *PeerJ Computer Science*, vol. 7, pp. 1–23, 2021, doi: 10.7717/PEERJ-CS.694.
- [14] V. Sampath, I. Maurtua, J. J. Aguilar Martín, and A. Gutierrez, *A survey on generative adversarial networks for imbalance problems in computer vision tasks*, vol. 8, no. 1. Springer International Publishing, 2021.
- [15] O. M. Elzeki, M. A. Elfattah, H. Salem, A. E. Hassaniien, and M. Shams, "A novel perceptual two layer image fusion using deep learning for imbalanced COVID-19 dataset," *PeerJ Computer Science*, vol. 7, pp. 1–35, 2021, doi: 10.7717/PEERJ-CS.364.
- [16] A. B. Nassif, I. Shahin, M. Bader, A. Hassan, and N. Werghi, "COVID-19 detection systems using deep-learning algorithms based on speech and image data," *Mathematics*, vol. 10, no. 4, pp. 1–25, 2022, doi: 10.3390/math10040564.
- [17] N. Danapaquiam et al., "A deep learning neural network techniques in visualization, imaging data acquisition and diagnosis for COVID-19," *Turcomat.Org*, vol. 12, no. 10, pp. 3226–3239, 2021.
- [18] H. U. R. Siddiqui et al., "An approach to detect chronic obstructive pulmonary disease using uwb radar-based temporal and spectral features," *Diagnostics*, vol. 13, no. 6, pp. 1–15, 2023, doi: 10.3390/diagnostics13061096.
- [19] S. U. Aswathy, P. P. F. Rajeena, A. Abraham, and D. Stephen, "Deep learning-based BoVW–CRNN model for lung tumor detection in nano-segmented CT images," *Electronics (Switzerland)*, vol. 12, no. 1, pp. 1–22, 2023, doi: 10.3390/electronics12010014.
- [20] R. Supriyanti, M. Alqaaf, Y. Ramadhani, and H. B. Widodo, "Morphological characteristics of X-ray thorax images of COVID-19 patients using the Bradley thresholding segmentation," *Indonesian Journal of Electrical Engineering and Computer Science (IJECS)*, vol. 24, no. 2, pp. 1074–1083, Nov. 2021, doi: 10.11591/ijeecs.v24.i2.pp1074-1083.
- [21] R. Supriyanti, M. R. Kurniawan, Y. Ramadhani, and H. B. Widodo, "Calculating the area of white spots on the lungs of patients with COVID-19 using the Sauvola thresholding method," *International Journal of Electrical and Computer Engineering (IJECE)*, vol. 13, no. 1, pp. 315–324, 2023, doi: 10.11591/ijece.v13i1.pp315-324.
- [22] R. Supriyanti, F. F. R. Wibowo, Y. Ramadhani, and H. B. Widodo, "Comparison of conventional edge detection methods performance in lung segmentation of COVID19 patients," *AIP Conference Proceedings*, vol. 2482, no. February, 2023, doi: 10.1063/5.0111683.
- [23] R. Supriyanti, "Technology supporting health services for rural areas based on image processing," in *Journal of Physics: Conference Series*, 2019, vol. 1367, no. 1, doi: 10.1088/1742-6596/1367/1/012090.
- [24] Rafael Gonzalez and Richard Woods, *Digital image processing*, 4th ed., vol. 1. New York: Pearson, 2017.
- [25] L. A. Samiadi and M. Yosia, "Rontgen Thorax," *Hello Sehat*, 2020.
- [26] H. E. Martz, C. M. Logan, D. J. Schneberk, and P. J. Shull, *X-Ray Imaging: Fundamentals, industrial techniques and applications*, 1st ed. Florida, United States: CRC Press, 2016.

BIOGRAPHIES OF AUTHORS



Retno Supriyanti    is a professor at Electrical Engineering Department, Jenderal Soedirman University, Indonesia. She received her Ph.D. in March 2010 from Nara Institute of Science and Technology Japan. Also, she received her M.S degree and Bachelor degree in 2001 and 1998, respectively, from Electrical Engineering Department, Gadjah Mada University Indonesia. Her research interests include image processing, computer vision, pattern recognition, biomedical application, e-health, tele-health and telemedicine. She can be contacted at email: retno_supriyanti@unsoed.ac.id.



Syadzwina Luke Dzihniza    received her Bachelor degree from Electrical Engineering Department, Jenderal Soedirman University Indonesia. Her research interest image processing field. She can be contacted at email: syadzwina.dzihniza@mhs.unsoed.ac.id.



Muhammad Alqaaf     received his Bachelor degree from Electrical Engineering Department, Jenderal Soedirman University Indonesia. MS. Degree in Nara Institute of Science and Technology Japan. Currently He is a Doctor Student in Nara Institute of Science and Technology Japan. His research interest image processing field and bioinformatics. He can be contacted at email: muhammad.alqaaf_subandoko.mb5@is.naist.jp.



Muhammad Rifqi Kurniawan    received his Bachelor degree from Electrical Engineering Department, Jenderal Soedirman University Indonesia. His research interest image processing field. He can be contacted at email: rifqikurniawan76@gmail.com.



Yogi Ramadhani     is an academic staff at Electrical Engineering Department, Jenderal Soedirman University, Indonesia. He received his MS Gadjah Mada University Indonesia, and his Bachelor degree from Jenderal Soedirman University Indonesia. His research interest including computer network, decision support system, telemedicine and medical imaging. He can be contacted at email: yogi.ramadhani@unsoed.ac.id.



Haris Budi Widodo     is an academic staff at Public Health Department, Jenderal Soedirman University, Indonesia. He received his Ph.D. from Airlangga University Indonesia. Also, He received his M.S degree and bachelor degree from Gadjah Mada University Indonesia. His research interest including public health, e-health and telemedicine. He can be contacted at email: haris.bwidodo@unsoed.ac.id.